

Is tailor-fitting always the best choice? The case of mutations in GISTs and Imatinib

S. Pricl¹, M. Ferrone¹, M.S. Paneni¹, E. Tamborini², S. Pilotti², M.A. Pierotti³

¹*Computer-aided System Laboratory, Department of Chemical, Environmental and Raw Materials Engineering, University of Trieste – Piazzale Europa 1, 34127 Trieste, Italy*
URL: www.caslab.units.it e-mail: sabrinap@dicamp.units.it

²*Experimental Molecular Pathology, Department of Pathology, Istituto Nazionale per lo Studio e la Cura dei Tumori, Via Venezian 1, 20133 Milano, Italy*

³*Department of Experimental Oncology, Istituto Nazionale per lo Studio e la Cura dei Tumori, Via Venezian 1, 20133 Milano, Italy*

Deregulation of c-kit has been implicated in the etiology of a number of cancers, including gastrointestinal stromal tumors (GISTs). Most of GISTs carry mutations in c-kit, resulting in an enhanced and constitutive ligand-independent tyrosine kinase activity that appears to play a key role in the pathogenesis of these tumors. Imatinib mesylate (STI571, Glivec[®], Gleevec[™]), a 2-phenylaminopyrimidine derivative, has shown remarkable efficacy in the treatment of GISTs, which are notoriously unresponsive to cancer chemotherapy. In this work we report the results obtained from a combined effort of bringing together clinical evidences on a newly discovered c-kit mutation in GISTs, showing acquired resistance to Imatinib, and a possible explanation, based on molecular simulations, of the mechanism by which this mutation may result in GISTs resistant to Imatinib.

Keywords: GISTs, Imatinib, mutations, c-kit, free energy calculations, binding energies, molecular modeling

1 INTRODUCTION

A new era of targeted cancer therapy was inaugurated with the approval of Imatinib mesylate (or STI 571/Gleevec) for the treatment of chronic myeloid leukemia (CML). STI-571 is a phenylaminopyrimidine compound, initially identified from a high-throughput screen for inhibitors of protein kinase C and subsequently found to be a potent and selective inhibitor of the Abl, platelet-derived growth factor β receptor, and kit tyrosine kinases [1]. Imatinib binds in a pocket close to the ATP-binding site of the Abl catalytic domain, and effectively inhibits Abl kinase activity *in vitro* and *in vivo* at concentrations of 0.1-1.0 μ M [2].

One year after its approval by FDA and EMEA for CML treatment, in 2001 Imatinib was also approved for advanced gastrointestinal stromal tumors (GISTs) chemotherapy. GISTs are the most common mesenchymal tumors of the gastrointestinal tract; they represent a spectrum of tumors, ranging from benign to highly malignant. The application of

Imatinib to GIST was a direct result of (1) its selective inhibition of the kit receptor tyrosine kinase, which is constitutively active in most GISTs, (2) its efficacy and minimal toxicity in patients with CML, (3) the parallels between the pathogenesis of GIST and CML, and (4) the lack of effective alternative treatments for metastatic GISTs.

In CML, Imatinib is highly effective both in early and late stages of the disease. Nonetheless, several relapses do occur after initial response, despite continued treatment [3]. In patients who developed resistance to Imatinib, reactivation of the Bcr-Abl signaling was observed, due to either a secondary mutation, resulting in a missense substitution of a residue belonging to the drug binding site and critical for binding, or to a progressive Bcr-Abl gene amplification [4]. In GISTs, primary resistance seems to involve at least 15% of patients with advanced disease, and its occurrence could be correlated with different c-kit mutations [5].

At the Istituto Nazionale per lo Studio e la Cura dei Tumori di Milano, among a series of 105 patients enrolled in a Phase III, prospective controlled trial on Imatinib in advanced GISTs, a point mutation in

exon 14, observed only in Imatinib nonresponding metastases, was identified for the first time. This mutation, T2030C, results in the corresponding protein mutation T670I, belonging to the ATP pocket of the kit receptor.

In this work, we present the results obtained from the application of combined detailed molecular modeling and experimental investigation techniques to the study of the interactions between T760I and Imatinib.

2 MODELING/EXPERIMENTAL DETAILS

2.1 Computational procedure

Since we verified an extremely high degree of homology between the ATP-binding pocket of Bcr-Abl and c-kit, we chose as a starting point the crystallized structure of Bcr-Abl in complex with Imatinib [6].

All calculations were carried out using the Amber 6.0 suite of programs [7] using the all-atoms force field by Cornell et al. [8]. All missing parameters for Imatinib were obtained performing ab initio calculations on a minimized structure. The corresponding partial charges were obtained using RESP [9]. To calculate the energetics of binding and examining the effects of conformational change and dynamics induced by the T315I mutation in Bcr-Abl (T760I in kit), we applied the following ansatz: binding free energies ΔG of Imatinib to wild type and T315I mutant Bcr-Abl were obtained by applying the so-called molecular mechanics Poisson-Boltzmann surface area (MM/PBSA) method of Kollman et al. [10]. To generate the mutant structure and estimate the relevant ΔG , we applied a method proposed by Reyes and Kollman [11], consisting in performing a separate molecular dynamics (MD) simulation on the mutated structure. Although more computationally expensive, this method gives more detailed insights on the structure and dynamics of the mutant. All energy analyses were performed separately for each complex and monomers of both mutant and wild type structures. The molecular mechanical energies were obtained with the anal module of the Amber 6.0 suite of programs, with the Cornell et al. force field. All intra-solute pairwise interactions were accumulated without a distance-based cut-off. Solvation free energy was estimated by continuum solvent methods as the sum of electrostatic and non-polar contributions. The first

were estimated by finite-difference solution of the Poisson-Boltzmann equation, as implemented in the Delphi package [12]. The non-polar contribution was estimated as a linear function of the solvent-accessible surface area, which implicitly includes the solute-solvent van der Waals interactions.

The mutation T315I was introduced to the wild type crystal structure of the Abl-Imatinib complex using InSighII (from Accelrys, San Diego CA, USA) by swapping the mutant residue into the specific site [13]. Starting mutant side chain orientation was selected using the side chain rotamer library method. Both the wild type and its mutant structure were relaxed using the sander module of Amber. We run 300 ps MD simulation of the T315I mutant complex at 300K with explicit water and counterions. A total of 25 snapshots from the mutant MD trajectory were then analyzed by MM/PBSA. The difference between the average mutant trajectory binding and wild type trajectory binding was calculated to yield the $\Delta\Delta G$ and standard deviations.

2.2 Experimental techniques

Morphologic, immunophenologic, molecular and biochemical analyses were carried out on resected lesions, two responding and one progressing. A c-kit mutational analysis on genomic DNA obtained from the tissue block of the primary tumor excised elsewhere was performed concomitantly. Immunostaining for CD117 was performed using the Dako antibody 1:250 diluted, following standard protocols. RNA and DNA were extracted, and the sequencing of the cDNA and genomic DNA was performed with an automated sequencing protocol, using kit sequence NCBI-#X06182 for comparison. Proteic extracts, immunoprecipitation experiments and Western Blotting analysis were performed according to standard procedures.

3 RESULTS AND DISCUSSION

3.1 Experimental evidences

The analysis of the entire c-kit cDNA sequence of the nonresponding metastases revealed a point mutation in exon 14, T2030C, resulting in the corresponding aminoacidic substitution T670I. This newly identified mutation, also confirmed at genomic level, was absent in the cDNA and genomic DNA from the corresponding metastases and from

the primary tumor. Strong cytoplasmatic CD117 positivity marked the non-responding lesion, while the responding ones showed weak cytoplasmic immunoreactivity. Immunoprecipitation and Western Blotting experiments paralleled this observation. In fact, the non-responding lesion showed a highly expressed and phosphorylated kit receptor, whereas the responding ones showed a weak it expression and activation, almost below the detection level.

3.2 Molecular modeling

Interestingly, our alignment of kit primary sequence with the aberrant tyrosine kinase expressed by the Philadelphia chromosome, Bcr-Abl, revealed that the mutation residue T760I corresponds to T315I of Abl receptor, an absolutely analogous mutation, which has been claimed to be the cause of acquired resistance to Imatinib in CML [14].

Mutating T to I at position 315 in the ATP binding domain of the Bcr-Abl receptor resulted in a calculated $\Delta\Delta G$ of binding of 1.74 kcal/mol with respect to the corresponding wild type structure [15]. This value is in a very good agreement with the corresponding experimental finding of 1.07 – 2.0 kcal/mol [16]. Figure 1 shows two snapshots extracted from the MD trajectory of the T760I mutant protein at the beginning and at the end (300 ps) of the simulation period, respectively.

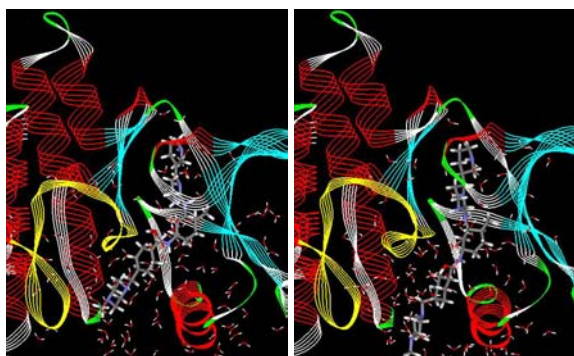


Fig. 1. Snapshots taken from the MD simulation of the T315I mutant at the beginning (left) and at the end (right) of the simulation period.

The analysis of the relevant trajectory clearly reveals that, with respect to the wild type system, the missing of the supposed-to-be critical H-bond [16] is not the only cause for the failing of receptor inhibition by Imatinib. Besides the obvious (and somewhat aleatory) dynamic nature of the water-mediated stabilizing interactions, we can see that the

interaction of the drug with the kit activation loop (white ribbon in bottom-left part of the figures) is drastically changed, the drug progressively drifting away from it during the considered time interval. In details, not only several of the wild type/Imatinib stabilizing H-bonds no longer exist in the mutant, but also a plethora of van der Waals and hydrophobic interactions are drastically, unfavorably changed in the mutant trajectory. As an example for all, the role played by the conformation of F382 of the well-conserved DFG motif, pointing towards the APT binding site (Figure 2, left), and thought crucial for the proper binding of Imatinib [6], is no longer maintained in the mutant trajectory, resulting in the net loss of a favorable stabilizing interaction.

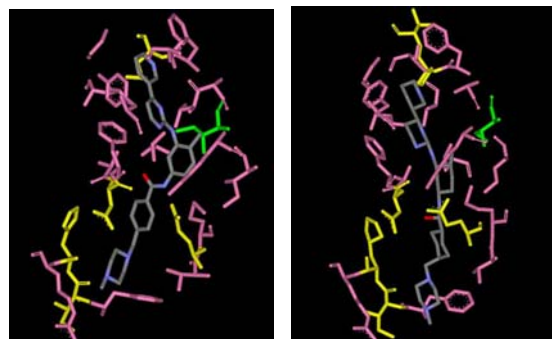


Fig. 2. ATP-binding pocket of T315I at the beginning (left) and at 300 ps (right) of MD simulation.

Some structural rearrangements in the conformation of the ATP-binding pocket of the kit-protein are clearly visible in Figure 2. Also, a modification of the activation loop can be envisaged, on the basis of the analysis of both wild type and mutant protein (see Figure 1), although longer simulations, being currently carried out by our group [17], are undoubtedly required to analyze these effects in details. These evidences would clearly, favorable support the hypothesis of Nagar et al. [6] that Imatinib requires a specific conformation of the kinase receptor before it can bind.

4 CONCLUSIONS

Exploiting the high homology of the ATP-binding pocket of c-kit in GISTs and Bcr-Abl in CML, we performed a preliminary molecular dynamics investigation of the binding of Imatinib to both wild type Bcr-Abl and its T315I mutant. Besides the good agreement between calculated and experimental DDG of binding, these experiments have highlighted

the fact that the presence of this mutation, as well that of its analogous T760I in GISTs, results in a distorted conformation of the ATP-binding pocket of the protein. This, in turn, confers to Imatinib a lesser ability to jam between the protein activation loop and helix α C, and hence to prevent the protein from assuming an active conformation.

ACKNOWLEDGMENTS

We acknowledge the generous financial support from AIRC, grant 2955 "Pathogenetic pathways determining pharmacological response: a novel tumoral functional classification approach" (2004). We are also grateful to UCSF for providing Amber 6.0.

The work is dedicated to the memory of Prof. Peter A. Kollman., deceased of cancer May, 2002.

BIBLIOGRAFIA

1. E. Buchdunger, J. Zimmermann, H. Mett, Z.T. Meyer, M. Muller, B.J. Druker, and N.B. Lindon, Inhibition of the Abl protein-tyrosine kinase in vitro and in vivo by a 2-phenylaminopyridimidine derivative, *Cancer Res.* 56 (1996) 100.
2. B.J. Druker, S. Tamura, E. Buchdunger, S. Ohno, G.M. Segal, S. Fanning, J. Zimmermann and N.B. London, Effects of a selective inhibitor of the Abl tyrosine kinase on the growth of Bcr-Abl positive cells., *Nat. Med.* 2 (1996) 561.
3. P. La Roseé, M.E. O'Dwyer and B.J. Druker, Insights from pre-clinical studies for new combination treatment regimens with the Bcr-Abl kinase inhibitor imatinib mesylate (Gleevec/Glivec) in chronic myelogenous leukemia: a translational perspective, *Leukemia* 16 (2002) 1213.
4. R. Nimmanapalli and K. Bhalla, Mechanisms of resistance to imatinib mesylate in Bcr-Abl-positive leukemias, *Curr. Opin. Oncol.* 14 (2002) 616.
5. S.I. Ernst, A.E. Hubbs, R.M. Przygodzki, T.S. Emory, L.H. Sobin and T.J. O'Leary, KIT mutation portends poor prognosis in gastrointestinal stromal/smooth muscle tumors, *Lab. Invest.* 78 (1998) 1633.
6. B. Nagar, W.G. Bornmann, P. Pellicena, T. Schindler, D.R. Veach, W.T. Miller, B. Clarkson and J. Kuriyan, Crystal structure of the kinase domain of c-Abl in complex with the small molecule inhibitors PDI173955 and Imatinib (STI-571), *Cancer Res.* 62 (2002) 4236.
7. D.A. Case, D.A. Pearlman, J.W. Caldwell, T.E. Cheatham III, W.S. Ross, C.L. Simmerling, T.A. Darden, K.M. Merz, R.V. Stanton, A.L. Cheng, J.J. Vincent, M. Crowley, V. Tsui, R.J. Radmer, Y. Duan, J. Pitera, I. Massova, G.L. Seibel, U.C. Singh, P.K. Weiner, P.A. Kollman, AMBER 6, (1999), University of California, San Francisco, CA, USA.
8. W. Cornell, P. Cieplak, C.I. Bayley, I. Gould, K.M. Merz, D.M. Ferguson, D.C. Spellmeyer, T. Fox, J.W. Caldwell and P.A. Kollman, A second generation force field for the simulation of proteins and nucleic acids, *J. Am. Chem. Soc.* 117 (1995) 5179.
9. C.I. Bayly, P. Cieplak, W.D. Cornell and P.A. Kollman, A well-behaved electrostatic potential based method using charge restraints for deriving atomic charges – the RESP model, *J. Phys. Chem.* 97 (1993) 10269.
10. J. Srinivasan, T. E. Chetham III, P. Cieplak, P.A. Kollman and D.A. Case, Continuum solvent studies of the stability of DNA, RNA and phosphoramidate-DNA helices, *J. Am. Chem. Soc.* 120 (1998) 9401.
11. C. Reyes and P.A. Kollman, Structure and thermodynamics of RNA-protein binding: using molecular dynamics and free energy analysis to calculate both the free energy of binding and conformational change, *J. Mol. Biol.* 297 (2000) 1145.
12. D. Sitkoff, K.A. Sharp and B. Honig, Accurate calculation of hydration free energies using macroscopic continuum models, *J. Phys. Chem.* 98 (1998) 1978.
13. S.C. Lovell, The penultimate rotamer library, *Proteins: Struct. Funct. Genet.* 40 (2000) 389.
14. M.E. Gorre, M. Mohammed, K. Ellwood, N. Hsu, R. Paquette, P.N. Rao and C.L. Sawyers, Clinical resistance to STI-571 cancer therapy caused by BCR-ABL gene mutation or amplification, *Science* 293 (2001) 876.
15. S. Pricl, A. Coslanich., M. Fermeglia, M. Ferrone, V. Albertini, L. Bonadiman, E. Tamborini, M. A. Pierotti and S. Pilotti, A tumor (GIST), a mutated gene (c-kit), and a molecular inhibitor (Imatinib): insight from computer simulations. In *Proceedings of the 2003 AICChE Annual Meeting*, November 16-21, San Francisco, CA, USA, (2003), CD ROM paper # 107g.
16. A.S. Corbin, E. Buchdunger, F. Pascal and B.J. Druker, Analysis of the structural basis of specificity of inhibition of the Abl kinase by STI-571, *J. Biol. Chem.* 35 (2002) 32214.
17. S. Pricl, M. Fermeglia, M. Ferrone, E. Tamborini and S. Pilotti, *Science* (2004), manuscript in preparation.